GEOPHYSICAL RESEARCH LETTERS, VOL 17, NO 10, PAGES 1657-1660, SEPTEMBER 1990

ELECTROSTATIC ELECTRON AND ION CYCLOTRON HARMONIC WAVES IN NEPTUNE'S MAGNETOSPHERE

D.D. Barbosa[1], W.S. Kurth[2], I.H. Cairns[2], D.A. Gurnett[2], R.L. Poynter[3]

Abstract. Voyager 2 observations of electrostatic electron and ion cyclotron waves detected in Neptune's magnetosphere are presented. Both types of emission appear in a frequency band above the electron and ion (proton) cyclotron frequencies, respectively, and are tightly confined to the magnetic equator occurring within a few degrees of it. The electron cyclotron waves are interpreted as electron Bernstein modes including an intense upper hybrid resonance emission excited by an unstable loss cone distribution of low-density superthermal electrons. The ion cyclotron waves are interpreted as hydrogen Bernstein modes including an intense lower hybrid resonance emission excited by an unstable ring distribution of low-density pickup N^+ ions deriving from the satellite Triton.

Introduction

One of the most persistent features of plasma waves found in planetary magnetospheres is the precise localization to the magnetic equator of intense electrostatic electron cyclotron harmonic (ECH) waves. These so-called $(n+\frac{1}{2})f_{ce}$ waves, as they have come to be known, have shown up consistently at all the magnetized planets and their tight confinement to the minimum $|\vec{B}|$ surface has provided a rather good diagnostic for the location of the magnetic equator. This feature has been unambiguously documented at Jupiter [Kurth et al., 1980], Saturn [Kurth et al., 1983], and Uranus [Kurth et al., 1986]. Terrestrial observations have also shown a clear preference of ECH waves for the magnetic equator [Fredericks and Scarf, 1973; Christiansen et al., 1978; Gough et al., 1979]. The recent Voyager 2 encounter with Neptune demonstrated that ECH waves are prominent features of all the giant planets and can reliably predict magnetic equator crossings in good agreement with direct independent measurements by the magnetometer [Gurnett et al., 1989; Ness et al., 1989].

While most discussion in the literature centers on electron cyclotron harmonic waves, there are also some measurements of ion cyclotron harmonic (ICH) waves associated with the magnetic equator. At Earth the observations of Gurnett (1976) and Olsen et al. (1987) have shown the common occurrence of (electromagnetic) waves at the equator with frequencies in a band just above the proton cyclotron frequency f_{cp}. Because of the much lower frequencies of ICH waves compared to ECH waves, their appearance in non-terrestrial magnetospheres has been severely limited due to the restricted frequency range of Voyager plasma wave instruments and to the restriction of most planetary encounter trajectories to spatial regions of the magnetosphere where the equatorial f_{cp} was very small and unobservable.

However, in one circumstance the closest approach distance of Voyager 1 at Jupiter coincided with a magnetic equator crossing at which time f_{cp} rose above the low-frequency threshold of the plasma wave receiver. During this period ICH waves were detected within a few degrees of the magnetic equator and the emissions were interpreted by Barbosa and Kurth (1990) as hydrogen Bernstein waves occurring at odd half-harmonic frequencies of the proton cyclotron frequency $(n+\frac{1}{2})f_{cp}$. The theoretical basis for the wave interpretation derived from previous studies of electrostatic wave phenomena in planetary magnetospheres which had an abundance of heavy ions in addition to magnetospheric protons [Barbosa, 1982; Barbosa et al., 1985]. Whereas the terrestrial ICH emissions have a significant magnetic component and have been interpreted as magnetosonic waves [Perraut et al., 1982], the Jovian ICH waves are considered more likely to be electrostatic emissions, i.e., Bernstein modes, because of the very low-β plasma conditions in which they occur [see Barbosa and Kurth (1990) for a full discussion of the electrostatic versus electromagnetic interpretation of planetary ICH waves]. The tight restriction of the ion Bernstein waves to the magnetic equator has the same explanation as that of electron Bernstein waves, i.e., the magnetic equator offers a preferred location for convective wave amplification in a dipole field geometry [Barbosa and Kurth, 1980; Barbosa, 1985].

The trajectory of Voyager 2 at Neptune was such that a magnetic equator crossing occurred sufficiently close to the planet ($r = 1.8\ R_N$) for f_{cp} to rise above the frequency threshold for detectability. A wave event was observed at this time with frequencies above f_{cp} and localized to a few degrees about the equator. This paper will describe the properties of both the electron waves and the ion waves interpreted here as hydrogen Bernstein waves at frequencies of $(n+\frac{1}{2})f_{cp}$. Neptune thus becomes the second outer planet along with Jupiter where ion waves of this class have been positively identified.

Electron Cyclotron Harmonic Waves

Figures 1a and 1b show data taken with the 16-channel plasma wave electric field spectrum analyzer on Voyager 2 during times when the spacecraft crossed the magnetic equator in the outer magnetosphere at distances of 10 R_N inbound (1a) and 11 R_N outbound (1b). From the centroid of the emission band one may estimate crossing times for the instantaneous (in the sense that some dynamical flapping of the plasma/neutral sheet

[1] Inst. of Geophysics and Planetary Physics, UCLA
[2] Dept. of Physics and Astronomy, Univ. of Iowa
[3] Jet Propulsion Laboratory

Copyright 1990 by the American Geophysical Union.

Paper number 90GL01024
0094-8276/90/90GL-01024$03.00

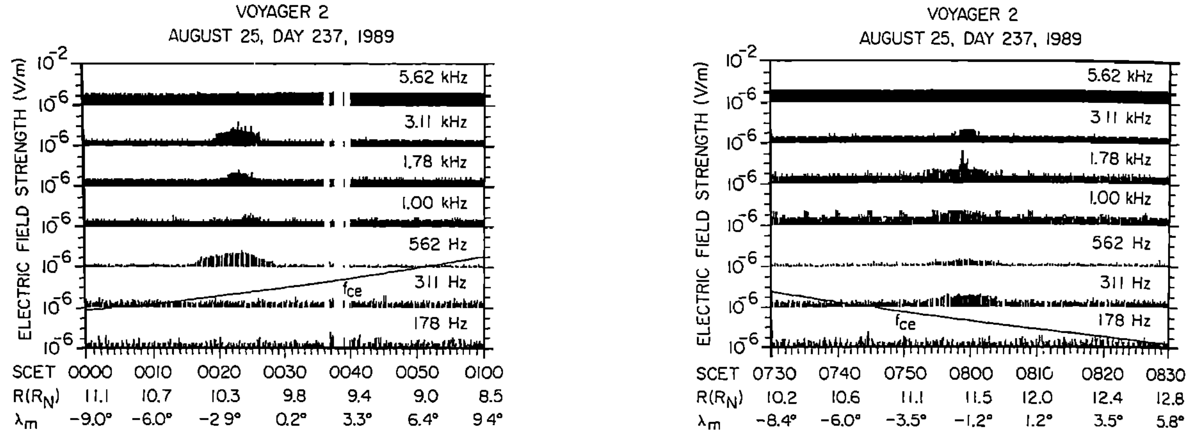

Fig. 1. 16-channel spectrum analyzer electric field amplitudes around the time of magnetic equator crossings (a) inbound near 10 R_N and (b) outbound near 11 R_N.

may be possible) magnetic equator of 237/0023 SCET inbound and 237/0759 outbound with an uncertainty of about ±2 mins. These times agree fairly well with predictions (viz., 237/0030 inbound and 237/0804 outbound) based on the offset tilted dipole (OTD) magnetic field model [Ness et al., 1989] but systematically preceed the OTD crossings by approximately 6 minutes.

Both events display all the signatures characteristic of ECH waves observed previously. The noise is confined to a band of frequencies above f_{ce} (shown as the solid curve in Figure 1 based on Voyager magnetometer data) which extends over several harmonics of f_{ce} with a distinct intensity maximum corresponding to a wave emission near the upper hybrid resonance (UHR) frequency which is identified as 3.11 kHz inbound and 1.78 kHz outbound. These UHR frequencies imply electron densities of 0.1 cm^{-3} and 0.04 cm^{-3} [Gurnett et al., 1989] which values are consistent with those measured by the plasma probe [Belcher et al., 1989].

The general theoretical interpretation of these noise bands is that they are electron Bernstein waves stimulated by a low-density superthermal population of electrons with a loss cone providing the source of instability [Barbosa and Kurth, 1980]. In situ electron measurements by Voyager have shown that a two-component (thermal and superthermal) electron distribution is present at Neptune occurring most prominently near the magnetic equator [Belcher et al., 1989] thus confirming general theoretical notions regarding the wave excitation mechanism albeit without any detailed information on the shape of the distribution and the free energy source. When convective amplification in an inhomogeneous dipole magnetic field is taken into account, the magnetic equator provides the most favorable conditions for large path-integrated growth with a very tight confinement of wave energy (± a few degrees) to the magnetic equator due to wave trapping [Barbosa, 1985]. It is also noted that the UHR emissions provide direct evidence in support of a linear mode conversion mechanism of upper hybrid waves to electromagnetic radiation that can explain the Voyager observations of periodic radio bursts at VLF frequencies from Neptune [Gurnett et al, 1989; Kurth et al, 1990].

Ion Cyclotron Harmonic Waves

Just after a pass at high planetographic latitudes around closest approach, Voyager 2 made another crossing of the magnetic equator deep inside the magnetosphere. The plasma experiment reported a large flux of hot ions and electrons at 237/0420 [Belcher et al., 1989] which corresponded to the time predicted for a magnetic equator crossing by the OTD model. At this time strong electric field signals were detected near and above the proton cyclotron frequency which we interpret as electrostatic ICH waves. The wave observations are depicted in Figure 2. The plot shows a special processing of 16-channel spectrum analyzer data which is usually displayed as fixed-frequency time profiles of electric field amplitude with 4 narrowband channels per decade of frequency. The data have been interpolated in frequency to create the equivalent of a colr spectrogram which has the advantage of showing all the plasma wave features in the best way for comparison purposes.

The ion wave event under discussion is evident at 0420 ± 2 mins. extending in frequency from the proton cyclotron frequency (white curve) $f_{cp} \approx$ 60 Hz up to about 400 Hz. The event shows a distinct cutoff at f_{cp} and is confined to ± 4° about the magnetic equator. This value is similar to that for electron waves (cf. Figure 1) and is virtually the same as that for all electrostatic cyclotron harmonic events found at all of the magnetized planets. This fact is a strong argument for the kinematic-geometrical basis of the equatorial localization of wave intensity [Barbosa and Kurth, 1980] and also for the generic similarity of ECH and ICH waves in terms of their common Bernstein mode structure. Some other low-frequency wave events are evident in the interval from 0400-0420 but the interpretation of these other waves is less obvious. The low-frequency noise below f_{cp} in the interval 0400-0410 may very well be ion cyclotron waves [Gurnett et al., 1989] while the other noise events appearing above f_{cp} may be a consequence of the complex magnetic field structure that exists at small radial distances due to substantial higher order magnetic field moments. Some of the noise at

∿ 200 Hz extending across the figure after 0425 is due to spacecraft interference.

Around this time high-resolution wideband data were available and a composite of several 48-second frames was shown in Figure 6 of Gurnett et al. (1989). It is evident from that figure that the low-frequency noise below 500 Hz in the 3 consecutive frames from 0418 to 0423 is extremely intense since all other noise at higher frequencies generally seen throughout the figure has been suppressed by the automatic gain control of the wideband receiver [Scarf and Gurnett, 1977]. In Figure 3 we show another version of the frame at 0420 with an expanded frequency scale. The spectrogram shows that there is a lot of fine structure to the noise consisting of narrowband features with an apparent harmonic structure very evident around 0420:27. The most prominent feature is the narrowband line emission at approximately 300 Hz.

The calibrated spectral density of these emissions is shown as the top two curves in Figure 4. The bottom curve marked "interference spectrum" shows for comparison the nominal level of spacecraft-associated noise thought to be associated with the operation of the tape recorder. The signal observed is ∿ 30 dB above the spacecraft noise level and is undoubtably real. The harmonic spacing between the peaks for the spectrum at 0420:23 is ∿ 80 Hz which is approximately the same as $f_{cp} \simeq 60$ Hz at this time; the small difference is possibly attributable to the finite frequency resolution $\Delta f \simeq 28$ Hz available in the wideband data (cf., Figure 3).

The top curve shows very clearly the prominent narrowband feature just below 300 Hz which we interpret as a lower hybrid emission. To verify this we note that in Figure 2 the upper frequency limit to the whistler mode noise, which decreases from 30 kHz to 10 kHz over the interval 0400-0420, can be identified as the electron plasma frequency. In this case the plasma density at 0420 is about 1 cm^{-3} which agrees with the plasma team's value [Belcher et al., 1989]. Assuming then that $f_{pe} \simeq 10$ kHz and $f_{ce} \simeq 110$ kHz, we estimate $f_{LHR} \simeq 230$ Hz for a proton-dominated plasma. This result bears a striking similarity to that of the LH emission found in the cold Io torus of Jupiter occurring just above f_{LHR} [Barbosa et al., 1985].

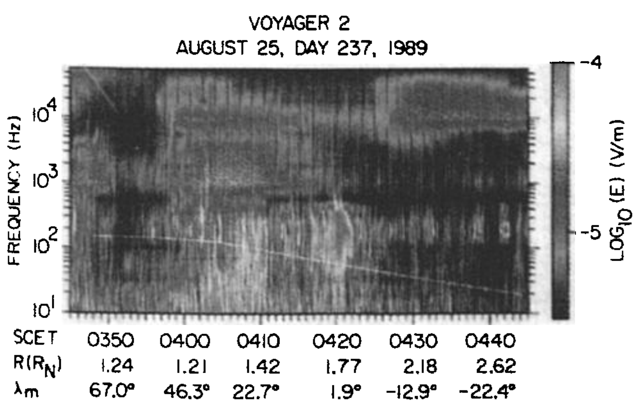

Fig. 2. color-coded spectrum analyzer data around the time of closest approach. The white curve is the proton cyclotron frequency f_{cp}.

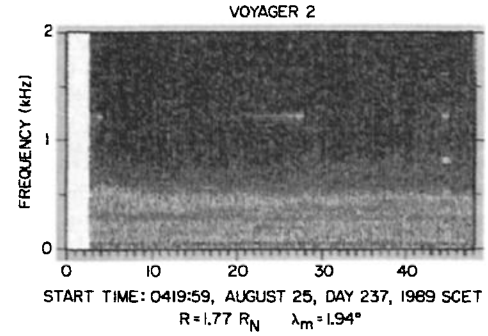

Fig. 3 high-resolution wideband data around the time of the magnetic equator crossing at 1.8 R_N.

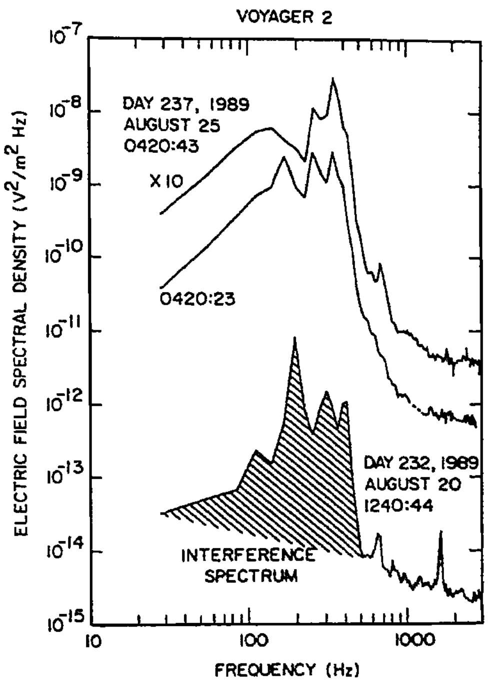

Fig. 4 calibrated spectral densities (top 2 curves) of the signal detected at 0420 SCET shown in Figure 3.

Conclusion

The Neptunian ECH waves are readily explained by the same theory proposed for ECH waves observed in other planetary magnetospheres: an unstable superthermal electron population leads to convective amplification of Bernstein modes with preferential conditions for growth at the magnetic equator. Electron measurements by the Voyager plasma experiment are consistent with this model.

The Neptunian ICH waves are explained in an analogous manner with an unstable distribution of heavy pickup ions (unmagnetized) providing growth to hydrogen Bernstein modes. It is our belief that the species of the heavy pickup ions is N^+ and their origin is the satellite Triton. If the ions are picked up at a distance L $\gtrsim$ 10, say, with a gyrospeed $V_o(L)$ and diffuse inwards, then at 1.8 R_N the peak of the pickup ring distribution will scale as $V(1.8) = V_o(L)(L/1.8)^{3/2} \sim 360$ km/s. The resultant energy of the hot N^+ ions is adequate to explain the ion spectra observed by the plasma team at 1.8 R_N [Belcher et al., 1989]; the radial diffusion process also maintains a sharp gradient $\partial f/\partial v_\perp$ in the positive slope region of the pickup ion distribution to counterbalance fill-in by quasilinear diffusion effects and to sustain large growth rates for the LH and Bernstein modes via the mechanism proposed by Barbosa and Kurth (1990).

The theory also allows us to gauge whether Doppler shift effects are important. According to Barbosa and Kurth (1990), the relative change in frequency is $\Delta f/f \sim V_{sc}/V \simeq 40/360 \sim 0.1$ for a spacecraft speed of roughly 40 km/s. Thus, Doppler smearing is not expected to be significant which explains why fine structure is present in Figure 3 when at Jupiter the effects of Doppler smearing were more apparent [Barbosa et al., 1985; Barbosa and Kurth, 1990]. Finally, the wavelength of the ICH waves may be estimated from pickup ion theory assuming that the wave phase speed is comparable to the characteristic speed V of the ring distribution. For the first harmonic band $\lambda \simeq V/f = 360/100 \sim 3$ km, and if such a value is to correspond to the proton gyroradius (the characteristic wavelength of hydrogen Bernstein waves) the proton temperature must be $T_H \simeq$ 700 eV, consistent with the results of Belcher et al. (1989).

Note added in proof. An updated version of the offset tilted dipole field model (OTD2) predicts magnetic equator crossings at 0023, 0421, and 0757 SCET which accord better with the crossing times specified by the ECH waves. Also, the radial component of the magnetic field B_r exhibits a sign reversal around 0423 SCET (N.F. Ness, private communication, 1990) which is in reasonable agreement with the occurrence time of the ICH event inasmuch as the general field configuration is quite complicated (non-dipolar) at such small radial distances.

Acknowledgements. We thank N.F. Ness and the Voyager magnetometer team for magnetic field measurements used herein. We also thank L.J. Granroth for invaluable assistance in the data reduction and graphic display. Support for this research was provided by NASA through grant NAGW-1558 and by NASA contract 957723 with the Jet Propulsion Laboratory.

References

Barbosa, D.D., Multi-ion resonances in finite temperature plasma, Astrophys. J., 254, 376, 1982.

Barbosa, D.D., Electrostatic wave propagation and trapping near the magnetic equator, Ann. Geophysicae, 3, 63, 1985.

Barbosa, D.D. and W.S. Kurth, Superthermal electrons and Bernstein waves in Jupiter's inner magnetosphere, J. Geophys. Res., 85, 6729, 1980.

Barbosa, D.D. and W.S. Kurth, Theory and observations of electrostatic ion waves in the cold Io torus, J. Geophys. Res., in press, 1990.

Barbosa, D.D., F.V. Coroniti, W.S. Kurth, and F. L. Scarf, Voyager observations of lower hybrid noise in the Io plasma torus and anomalous plasma heating rates, Astrophys. J., 289, 392, 1985.

Belcher, J.W. et al., Plasma observations near Neptune: initial results from Voyager 2, Science, 246, 1478, 1989.

Christiansen, P.J. et al., Geos-1 observations of electrostatic waves and their relationship with plasma parameters, Space Sci. Rev., 22, 383, 1978.

Fredericks, R.W. and F.L. Scarf, Recent studies of magnetospheric electric field emissions above the electron gyrofrequency, J. Geophys. Res., 78, 310, 1973.

Gough, M.P., P.J. Christiansen, G. Martelli, and E.J. Gershuny, Interaction of electrostatic waves with warm electrons at the geomagnetic equator, Nature, 279, 515, 1979.

Gurnett, D.A., Plasma wave interactions with energetic ions near the magnetic equator, J. Geophys. Res., 81, 2765, 1976.

Gurnett, D.A. et al., First plasma wave observations at Neptune, Science, 246, 1494, 1989.

Kurth, W.S., D.D. Barbosa, D.A. Gurnett, and F.L. Scarf, Electrostatic waves in the Jovian magnetosphere, Geophys. Res. Lett., 7, 57, 1980.

Kurth, W.S., F.L. Scarf, D.A. Gurnett, and D.D. Barbosa, A survey of electrostatic waves in Saturn's magnetosphere, J. Geophys. Res., 88, 8959, 1983.

Kurth, W.S., D.D. Barbosa, D.A. Gurnett, and F.L. Scarf, Electrostatic waves in the magnetosphere of Uranus, J. Geophys. Res., 92, 15225, 1987.

Kurth, W.S., D.D. Barbosa, D.A. Gurnett, R.L. Poynter, and I.H. Cairns, Low-frequency radio emissions at Neptune, Geophys. Res. Lett., this issue, 1990.

Ness, N.F. et al., Magnetic fields at Neptune, Science, 246, 1474, 1989.

Olsen, R.C. et al., Plasma observations at the earth's magnetic equator, J. Geophys. Res., 92, 2385, 1987.

Perraut, S. et al., A systematic study of ULF waves above F_{H^+} from GEOS 1 and 2 measurements and their relationship with proton ring distributions, J. Geophys. Res., 87, 6219, 1982.

Scarf, F.L. and D.A. Gurnett, A plasma wave investigation for the Voyager mission, Space Sci. Rev., 22, 687, 1977.

D.D. Barbosa, Institute of Geophysics and Planetary Physics, UCLA, Los Angeles, CA 90024.

I.H. Cairns, D.A. Gurnett, and W.S. Kurth, Department of Physics and Astronomy, University of Iowa, Iowa City, IA 52242.

R.L. Poynter, Jet Propulsion Laboratory, 4800 Oak Grove Drive, Pasadena, CA 91109.

(Received April 2, 1990;
accepted April 24, 1990.)